Macromolecules **1996,** *29,* 5843−5851

Miscibility, Thermal Properties, and Enzymatic Degradability of Binary Blends of Poly[(*R*)-3-hydroxybutyric acid] with Poly(ϵ-caprolactone-*co*-lactide)

Naoyuki Koyama and Yoshiharu Doi*

Polymer Chemistry Laboratory and the RIKEN Group of the Research Institute of Innovative Technology for the Earth (RITE), The Institute of Physical and Chemical Research (RIKEN), Hirosawa 2-1, Wako-shi, Saitama 351-01, Japan

Received January 25, 1996; Revised Manuscript Received May 3, 1996⊗

ABSTRACT: The miscibility, morphology, and biodegradability of binary blends of poly[(*R*)-3-hydroxybutyric acid] (P[(*R*)-3HB]) ($M_n = 300\,000$) with poly(ϵ-caprolactone-*co*-lactide) (P(CL-*co*-LA)) ($M_n = 1500-40\,000$) have been studied by means of differential scanning calorimetry (DSC), optical microscopy, scanning electron microscopy (SEM), enzymatic hydrolysis, and biodegradation in river water. Copolymers of ϵ-caprolactone (CL) and (*R*,*S*)-lactide (LA) with a wide range of compositions were prepared by ring-opening copolymerization of ϵ-caprolactone with (*R*,*S*)-lactide in the presence of aluminum triisopropoxide as an initiator. The P(CL-*co*-LA) samples were found to have a random sequence distribution of monomer units by ^{13}C NMR analysis. The P(CL-*co*-LA) films were hydrolyzed by a lipase from *Rhizopus delemar*, and the rates of enzymatic hydrolysis were higher than that of PCL homopolymer. DSC analysis revealed that the solid-state structure of P[(*R*)-3HB]/P(CL-*co*-LA) blends was strongly dependent on the copolymer composition of the P(CL-*co*-LA) component. The miscible blends of P[(*R*)-3HB] were prepared with amorphous P(CL-*co*-LA) ranging from 30 to 100 mol % LA. The spherulites of P[(*R*)-3HB] in the miscible P[(*R*)-3HB]/P(CL-*co*-LA) blends were volume-filled, and the spherulitic growth rate decreased with an increase in the content of the P(CL-*co*-LA) component. The enzymatic hydrolysis of P[(*R*)-3HB]/P(CL-*co*-LA) blend films was carried out at 37 °C and pH 7.4 in a potassium phosphate buffer with an extracellular PHB depolymerase from *Alcaligenes faecalis*. The rates of enzymatic hydrolysis on the films of P[(*R*)-3HB]/P(CL-*co*-LA) blends decreased with an increase in the P(CL-*co*-LA) content.

Introduction

A wide variety of bacteria accumulate an optically active polymer of (*R*)-3-hydroxybutyric acid as an intracellular storage material of carbon and energy source.[1,2] Poly[(*R*)-3-hydroxybutyric acid] (P[(*R*)-3HB]) isolated from bacteria is a biodegradable and biocompatible thermoplastic with a melting temperature around 180 °C.[2,3] Bacterial P[(*R*)-3HB] has attracted industrial attention as an environmentally degradable plastic for a wide range of agricultural, marine, and medical applications. However, bacterial P[(*R*)-3HB] is a highly crystalline and brittle material. Some attempts have been made to improve its physical properties by means of blending with other biodegradable polymers. Poly(ethylene oxide),[4,5] cellulose esters,[6,7] and atactic poly[(*R*,*S*)-3-hydroxybutyric acid][8−10] have been found to be miscible with bacterial P[(*R*)-3HB].

Poly[(*S*)-lactide] (P[(*S*)-LA]) has been investigated as a material for medical devices such as controlled drug release matrixes, degradable sutures, and implants for bone fixation.[11] Although it has been reported that some enzymes hydrolyze P[(*S*)-LA],[12,13] the degradation of P[(*S*)-LA] in an aqueous environment is mainly due to nonenzymatic hydrolysis of polymer chains catalyzed by carboxyl end groups of polymers.[14] On the other hand, poly(ϵ-caprolactone) (PCL) is known to be an enzymatic degradable polyester hydrolyzed by lipases from many microorganisms.[15] Thus, the binary blends of P[(*R*)-3HB]/P[(*S*)-LA] and P[(*R*)-3HB]/PCL are anticipated to be completely degradable. The miscibility and morphology of the blends of P[(*R*)-3HB]/PCL[16] and P[(*R*)-3HB]/P[(*R*,*S*)-LA][17] have been investigated in our laboratory. The blend of bacterial P[(*R*)-3HB] ($M_n = 360\,000$) with PCL ($M_n = 36\,000$) was immisible,[16] while the blend of P[(*R*)-3HB] ($M_n = 300\,000$) with P[(*R*,*S*)-LA] ($M_n = 9000$) was miscible in the melt and in the amorphous state.[17] In this paper, we prepare copolymers of ϵ-caprolactone and (*R*,*S*)-lactide P(CL-*co*-LA) with a wide range of copolymer composition and molecular weight and investigate the miscibility, morphology, and biodegradability of binary blends of bacterial P[(*R*)-3HB] ($M_n = 300\,000$) with P(CL-*co*-LA) by means of differential scanning calorimetry, optical microscopy, scanning electron microscopy, enzymatic hydrolysis, and biodegradation in river water.

Experimental Section

Materials. The bacterial P[(*R*)-3HB] ($M_n = 300\,000$, $M_w = 650\,000$) sample was purchased from Aldrich Chemical Co. The P[(*R*)-3HB] sample was purified by precipitation in hexane from chloroform solution at room temperature and dried *in vacuo* for 2 days.

Preparation of P(CL-*co*-LA). Poly(ϵ-caprolactone-*co*-lactide) (P(CL-*co*-LA)) samples were prepared by ring-opening copolymerization of ϵ-caprolactone with (*R*,*S*)-lactide according to the method of Teyssie *et al.*[18,19] ϵ-Caprolactone from Wako Chemicals was dried over CaH_2 under nitrogen at room temperature for 1 day and distilled under reduced pressure. (*R*,*S*)-Lactide (PURAC biochem.) was recrystallized two times from dried toluene at 60 °C and dried *in vacuo* for 1 day. Aluminum triisopropoxide ($Al(O^iPr)_3$; Kanto Chemical) was purified by distillation under reduced pressure and dissolved in dried toluene. Copolymerizations of ϵ-caprolactone with (*R*,*S*)-lactide were carried out in toluene with $Al(O^iPr)_3$ as an initiator at 70 °C for 5 days. The monomer concentrations were 1 mol/L, and mole ratios of monomer to initiator were in the range 50−600. The produced polymer was recovered by precipitation in ether/hexane (90/10) and dried under reduced pressure at room temperature.

P(CL-*co*-LA) samples of low molecular weights were prepared by methanolysis.[20] The copolymer (1 g) was dissolved in chloroform (30 mL) in a 50 mL screw bottle, and 10 mL of

---

* Author to whom correspondence should be addressed.

⊗ Abstract published in *Advance ACS Abstracts,* July 15, 1996.

S0024-9297(96)00119-2 CCC: $12.00

3 vol/vol % sulfuric acid in methanol was added. The bottle was kept at 35 °C for 1 h. The reaction solution was neutralized by addition of 5 wt/wt % sodium bicarbonate solution. The organic layer was dried under anhydrous magnesium sulfate, precipitated 10 times in diethyl ether, recovered, and dried under reduced pressure at room temperature.

Preparation of Blend Films. Blend films (~0.05 mm thickness) were prepared by conventional solution-casting techniques from chloroform solutions (20 mg/mL) of P[(*R*)-3HB] and P(CL-*co*-LA) samples using glass Petri dishes as casting surfaces. The viscosities of chloroform solutions were not adjusted for the preparation of blend films. The films were dried to constant weight *in vacuo* and then aged at least 3 weeks at room temperature to reach equilibrium crystallinity prior to analysis.

Enzymatic Degradation. The extracellular lipase from *Rhizopus delemar* was purchased from Seikagaku Kogyo (Tokyo) and used without further purification. The extracellular PHB depolymerase was purified to electrophoretic homogeneity from *Alcaligenes faecalis* T1.[21] The enzymatic hydrolysis of solution-cast films of P(CL-*co*-LA) and of P[(*R*)-3HB]/P(CL-*co*-LA) blends were carried out at 37 °C in 0.1 M potassium phosphate buffer (pH 7.4). Films (initial weights, ~5 mg; initial film dimensions, 10 × 10 × 0.05 mm) were placed in small bottles containing 1.0 mL of phosphate buffer. The reaction was started by the addition of an aqueous solution of lipase (500 μg) or PHB depolymerase (1.5 μg). The reaction solution was incubated at 37 ± 0.1 °C with shaking. Sample films were removed after reaction, washed with distilled water, and dried to constant weight *in vacuo*. The weight loss data were averaged on three film samples.

Biodegradation in River Water. The biodegradation test was a modified version of the MITI test.[22] All tests were performed under aerobic conditions in a temperature-controlled BOD tester (TAITEC O_2 up tester 10B) at 25 °C with stirring. A sample film (initial weight, ~10 mg; initial thickness, 0.05 mm) was placed in a 300 mL BOD reactor, and 200 mL of natural water from the Arakawa river (Saitama, Japan) was added. A mineral salt solution (0.2 mL) was added to the river water, which contained the following (per liter): 8.50 g of KH_2PO_4, 21.75 g of K_2HPO_4, 33.30 g of$Na_2HPO_4 \cdot 2H_2O$, 1.70 g of NH_4Cl, 22.50 g of $MgSO_4 \cdot 7H_2O$, 27.50 g of $CaCl_2$, and 0.25 g of $FeCl_3 \cdot 6H_2O$. The biodegradation test was carried out at 25 °C for 28 days, and the biochemical oxygen demand (BOD) was measured continuously with a BOD meter. Sample films were removed after 28 days, washed with distilled water, and dried to constant weight *in vacuo*. The BOD biodegradability of the sample was calculated by subtracting the biochemical oxygen demand of the control blank (BOD_b) from that of test solution (BOD_t) and dividing the value ($BOD_t - BOD_b$) by the theoretical oxygen demand (ThOD) of the test sample.

Analytical Procedures. The ^1H and ^{13}C NMR analyses of P(CL-*co*-LA) samples were carried out on a JEOL α-400 spectrometer. The 400-MHz ^1H NMR spectra were recorded at 27 °C in a $CDCl_3$ solution of P(CL-*co*-LA) (5 mg/mL) with a 4.7 μs pulse width (45° pulse angle), 3 s pulse repetition, 8000 Hz spectral width, 16K data points, and 16 scans. The 100-MHz ^{13}C NMR spectra were recorded at 27 °C in a $CDCl_3$ solution of P(CL-*co*-LA) (30 mg/mL) with a 4.1 μs pulse width (45° pulse angle), 5 s pulse repetition, 27 000 Hz spectral width, 16K data points, and 12 000 scans. Tetramethylsilane (Me_4Si) was used as an internal chemical shift standard.

All molecular weight data were obtained by gel-permeation chromatography at 40 °C, using a Shimadzu 6A GPC system and a 6A refractive index detector with Shodex K-80M and K-802 columns. Chloroform was used as eluent at a flow rate of 0.8 mL/min, and sample concentrations of 1.0 mg/mL were applied. Polystyrene standards with a low polydispersity were used to make a molecular weight calibration curve.

The differential scanning calorimetry (DSC) data of samples were recorded in the temperature range −100 to +200 °C under a nitrogen flow of 30 mL/min on a Shimadzu DSC-50Q instrument equipped with a cooling accessory. The solution-cast films (3 mg) were encapsulated in aluminum pans and heated from 0 to 200 °C at a rate of 10 °C/min (first scan). The peak melting temperature (T_m) and enthalpy of fusion (ΔH_m) were determined from the DSC endotherms. For measurement of the glass-transition temperature (T_g), the samples were maintained at 200 °C for 1 min and then rapidly quenched at −100 °C. They were then heated from −100 to +200 °C at a heating rate of 20 °C/min (second scan). The T_g was taken as the midpoint of the heat capacity change. The cold crystallization peak temperature (T_{cc}) was determined from the DSC exotherm.

The morphologies of P[(*R*)-3HB] spherulites were observed with an optical microscope (Nikon OPTIPHOTO-2) equipped with crossed polarizers, a Linkam hot stage, a CCD camera (Ikegami IF-8500), and an image analyzer (OLYMPUS XL-10). The solution-cast film (1 mg) of the P[(*R*)-3HB]/P(CL-*co*-LA) blend was first heated on a hot stage from room temperature to 200 °C at a rate of 30 °C/min. The sample was maintained at 200 °C for 30 s, and then the temperature was rapidly lowered to a given crystallization temperature (T_c) of 60−120 °C. The sample was crystallized isothermally at a given T_c to monitor the growth of spherulites as a function of time. The radial growth rate of P[(*R*)-3HB] spherulites was calculated as the slope of the line obtained by plotting the spherulite radius against time with more than ten data points.

The surfaces of sample films were observed with a scanning electron microscope (JEOL JSM5300) after gold coating of samples using an ion sputtering device (JEOL JFC-1100E).

The dissolved organic carbon concentration (DOC) of the biodegradation test solution was determined on a Shimadzu TOC-5000.

Results and Discussion

Synthesis and Characterization of P(CL-*co*-LA). Syntheses of P(CL-*co*-LA) samples were carried out by ring-opening copolymerization of ϵ-caprolactone (ϵ-CL) and (*R*,*S*)-lactide (LA) with aluminum triisopropoxide as an initiator. Table 1 lists the copolymer compositions, yields, thermal properties, and molecular weights of the produced P(CL-*co*-LA) samples (1−22). The copolymer compositions of P(CL-*co*-LA) were in good agreement with monomer feed ratios, independent of copolymer yield. Number-average molecular weights (M_n) of the copolymers increased from 1500 to 40 000 with an increase in the mole ratio of monomer/initiator. Polydispersities of molecular weights were in the range 1.4−4.4. Controlled methanolysis was employed to prepare the P(CL-*co*-LA) samples (23 and 24) with M_n values of 6900 (see Table 1).

Figure 1 shows the effects of copolymer composition on the thermal properties of the P(CL-*co*-LA) samples. The homopolymer (PLA) of (*R*,*S*)-lactide was an amorphous polymer, while the homopolymer (PCL) of ϵ-caprolactone was a partially crystalline polymer with a melting temperature (T_m) around 60 °C. The incorporation of LA units into the PCL chain resulted in a decrease of T_m, and no enthalpy of fusion was detected in the samples with copolymer compositions over 21 mol % of LA unit. The glass-transition temperature (T_g) increased from −67 to +49 °C with increasing LA content.

^{13}C NMR analyses were performed to determine the monomer sequence distributions of the P(CL-*co*-LA) samples. Figure 2 shows a 100-MHz ^{13}C NMR spectrum of P(CL-*co*-75 mol % LA) (sample 22), together with the chemical shift assignment for each carbon resonance. The expanded carbonyl carbon resonances at 169.1−173.5 ppm (from Me_4Si) in Figure 2 were resolved into several peaks due to triad sequences of caprolactone (C) and half-lactide (lactic acid) (L) units. The chemical shift assignment of the carbonyl carbon resonances was made according to previous papers.[18,23] It is of interest

Table 1. Thermal Properties and Molecular Weights of Copolymers Obtained by Copolymerizations of ε-Caprolactone (CL) and (*R*,*S*)-Lactide (LA) in Toluene with Al(O^iPr)$_3$ at 70 °C for 5 days

sample no.	monomer feed ratio, mol %		comp in polymer,[a] mol %		monomer/ initiator, mol/mol	yield, %	T_g,[b] °C	T_m,[c] °C	ΔH_m,[d] J/g	mol wt[e]	
	CL	LA	CL	LA						$10^{-3}M_n$	M_w/M_n
1	89	11	87	13	50	7	−58	15, 38	10, 9	1.5	3.5
2	75	25	79	21	50	7	−49	nd[f]	0	1.7	3.0
3	75	25	80	20	50	11	−51	nd	0	1.7	4.4
4	57	43	55	45	50	9	−24	nd	0	1.8	3.9
5	33	67	37	63	50	20	−6	nd	0	1.8	3.0
6	89	11	93	7	100	59	−55	50	60	15	1.7
7	75	25	80	20	100	59	−48	nd	0	14	1.8
8	57	43	59	41	100	54	−21	nd	0	17	1.4
9	33	67	31	69	100	69	8	nd	0	11	1.9
10	0	100	0	100	100	96	40	nd	0	19	1.5
11	100	0	100	0	200	83	−67	60	110	22	2.2
12	89	11	91	9	200	72	−52	48	53	19	1.8
13	80	20	82	18	254	78	−48	20, 39	2, 4	24	1.8
14	75	25	79	21	200	70	−45	nd	0	23	1.8
15	57	43	59	41	200	48	−23	nd	0	22	1.6
16	33	67	32	68	200	32	12	nd	0	18	1.8
17	0	100	0	100	200	98	49	nd	0	17	2.1
18	100	0	100	0	600	75	nd	61	102	28	1.6
19	89	11	90	10	600	85	−57	46	42	37	2.5
20	75	25	73	27	600	68	−40	nd	0	30	2.0
21	57	43	58	42	600	79	−23	nd	0	33	1.6
22	33	67	25	75	600	71	19	nd	0	40	1.6
23[g]	methanolysis of 20		70	30			−45	nd	0	6.9	2.2
24[g]	methanolysis of 21		59	41			−28	nd	0	6.9	2.5

[a] Determined from ^{1}H-NMR spectra. [b] Glass-transition temperature. [c] Melting temperature. [d] Enthalpy of fusion measured by DSC (first scan). [e] Determined by GPC analysis. [f] Not detected. [g] Samples 23 and 24 were obtained by the controlled methanolysis of samples 20 and 21, respectively.

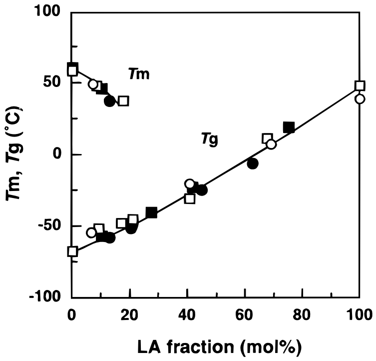

Figure 1. Thermal properties of P(CL-*co*-LA) with different copolymer composition. Copolymers were obtained at monomer/ initiator ratios (mol/mol) of 50 (●), 100 (○), 200 (□), and 600 (■), respectively.

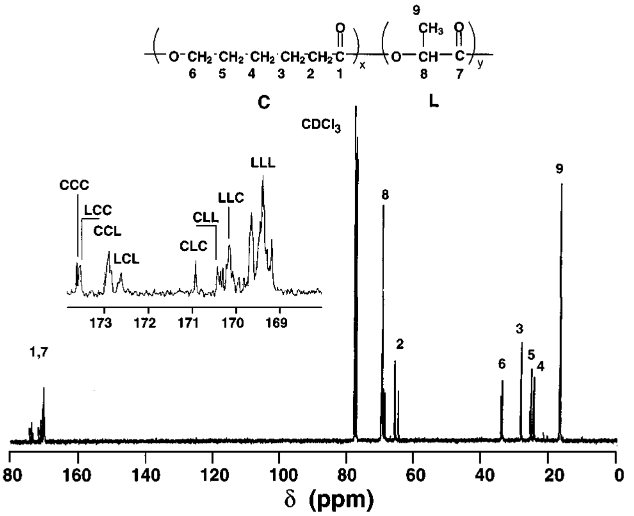

Figure 2. 100-MHz ^{13}C NMR spectrum of P(CL-*co*-75 mol % LA) copolymer (sample 22) in $CDCl_3$ at 23 °C.

to note that the CLC triad peak appears in Figure 2. If ε-caprolactone and lactide were simply copolymerized, the fraction of CLC triad sequence should be negligible. The presence of the CLC triad sequence indicates that transesterification took place during the copolymerization.[24]

The triad fractions were calculated from the relative peak areas of the carbonyl resonances. Table 2 lists the triad fractions of four copolymer samples (19−22), together with the ^{13}C chemical shift assignment. The triad sequence distribution data for two monomeric units were compared with the Bernoullian statistics applicable to a statistically random copolymerization of caprolactone (C) with lactic acid (L) units. In the Bernoullian model, the mole fraction F_{iji} of triad sequence *iji* can be expressed with the mole fractions F_i and F_j of *i* and *j* units as $F_{iji} = F_i2\,F_j$. As shown in Table 2, the calculated triad fractions are in agreement with the observed values for four samples, suggesting that the P(CL-*co*-LA) samples have random sequence distributions of caprolactone and lactic acid (half-lactide) units.

The enzymatic hydrolysis of six P(CL-*co*-LA) samples (17−22) were carried out with the solution-cast films in the aqueous solution of a lipase at 37 °C and pH 7.4. In this study, an extracellular lipase from *Rhizopus delemar* was used because the lipase is known to hydrolyze PCL.[25] The weight loss of the film was measured as a function of time for 36 h and was found to increase proportionally with time. The rate of enzymatic degradation was determined from the slope of the line obtained by the weight loss against time. Figure 3 shows the rates of enzymatic hydrolysis of P(CL-*co*-LA) films by the lipase. No weight loss was observed on the film of PLA homopolymer (sample 17),

Table 2. Chemical Shifts and Relative Intensities of Carbonyl Carbon Resonances in P(CL-*co*-LA) Samples

		relative intensities[b] of samples 19, 20, 21, and 22			
chem shift, ppm	sequence[a]	19	20	21	22
173.56 173.49	CCC + LCC	0.70 (0.66)	0.51 (0.32)	0.23 (0.17)	0.06 (0.02)
172.90 172.81	CCL + LCL	0.17 (0.15)	0.17 (0.25)	0.17 (0.23)	0.13 (0.12)
170.88	CLC	0.13 (0.12)	0.12 (0.14)	0.08 (0.10)	0.03 (0.02)
170.38 170.10	CLL + LLC	0.00 (0.06)	0.20 (0.21)	0.22 (0.29)	0.19 (0.21)
169.77 169.15	LLL	0.00 (0.01)	0.00 (0.08)	0.30 (0.21)	0.59 (0.63)

[a] C and L denote caprolactone and half-lactide (lactic acid) units, respectively. [b] The values in parentheses were calculated by Bernoullian statistics.

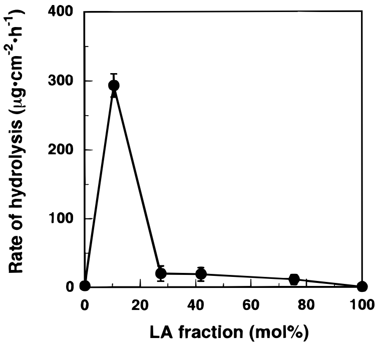

Figure 3. Effect of copolymer composition on the rate of enzymatic hydrolysis of P(CL-*co*-LA) films in the aqueous solution of lipase from *R. delemar* at 37 °C and pH 7.4.

and the rate of enzymatic hydrolysis on the film of PCL homopolymer (sample 18) was as low as 1.8 ± 0.2 μg$\cdot$cm$^{-2}\cdot$h^{-1}. The rates of enzymatic hydrolysis for the films of P(CL-*co*-LA) copolymer samples 19−22 were higher than the rate of PCL homopolymer. The highest rate (293 ± 17 μg$\cdot$cm$^{-2}\cdot$h^{-1}) was observed for P(CL-*co*-10 mol % LA) film, and the rate was ~160 times faster than that of PCL homopolymer. In a previous paper,[26] we studied the enzymatic degradation of random copolymers of ϵ-caprolactone (CL) with (*R*)-β-butyrolactone (3HB) in the presence of a lipase from *R. delemar* and reported that the highest rate of enzymatic hydrolysis by lipase was observed on the solution-cast film of P(CL-*co*-9 mol % 3HB). The weight loss profile of P(CL-*co*-LA) films by lipase was similar to that of P(CL-*co*-3HB) film against the copolymer composition. These results suggest that the rate of enzymatic hydrolysis is regulated not only by the crystallinity of the polymer but also by the chemical structure of the monomeric units and the substrate specificity of lipase.[26]

Thermal Properties and Miscibility of P[(*R*)-3HB]/P(CL-*co*-LA) Blends. The glass-transition temperature (T_g), cold crystallization peak temperature (T_{cc}), melting temperature (T_m), and enthalpy of fusion (ΔH_m) of binary blends of P[(*R*)-3HB] (M_n = 300 000) with P(CL-*co*-LA) (M_n = 17 000−24 000) of different copolymer compositions (samples 11−17) were determined from DSC thermograms. The results are summarized in Table 3.

Figure 4 shows typical DSC thermograms (second scan) of miscible and immiscible blends. The T_g values of P[(*R*)-3HB] and P(CL-*co*-18 mol % LA) (sample 13) were respectively +4 and −48 °C, and the T_g values of both components in the P[(*R*)-3HB]/P(CL-*co*-18 mol % LA) blend were almost independent of the blend composition (see Figure 4a), indicating that the binary blend is immiscible in the melt. In contrast, the blend of P[(*R*)-3HB] with P(CL-*co*-41 mol % LA) (sample 15) showed a single T_g, and the T_g value was dependent on the blend composition (see Figure 4b), indicating that the binary blend is miscible in the melt. This result suggests that the miscibility of the P[(*R*)-3HB]/P(CL-*co*-LA) blend is influenced by the copolymer composition of P(CL-*co*-LA) component.

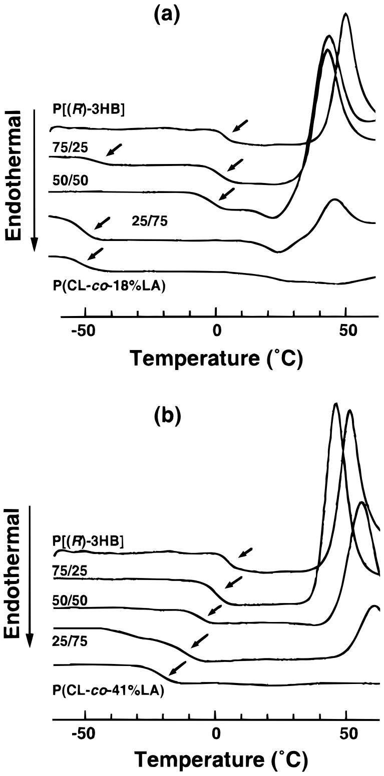

Figure 4. DSC thermograms (second scan) of P[(*R*)-3HB]/P(CL-*co*-LA) blends at a rate of 20 °C/min; (a) blend of P[(*R*)-3HB] with P(CL-*co*-18 mol % LA) (M_n = 24 000), sample 13; (b) blend of P[(*R*)-3HB] with P(CL-*co*-41 mol % LA) (M_n = 18 000), sample 15.

As Table 3 shows, the blends of P[(*R*)-3HB] and P(CL-*co*-LA) (samples 11−14) with LA fractions ranging from 0 to 21 mol % exhibited two T_g values characteristic of the blend components, indicating that the blends of P[(*R*)-3HB] and P(CL-*co*-LA) with 0−21 mol % LA are immiscible in the melt. In contrast, the blend of P[(*R*)-3HB] with P(CL-*co*-41 mol % LA) (sample 15) showed a single T_g, and the value of T_g was dependent on the blend composition. The T_g values were in good agreement with the curve calculated with the *k* value of 0.78 by the Wood's equation:[27]

$$T_g = (w_1 T_{g_1} + k w_2 T_{g_2})/(w_1 + k w_2) \qquad (1)$$

where w_1 and w_2 are the weight fractions, T_{g1} and T_{g2} are respectively the glass-transition temperatures of the P[(*R*)-3HB] and P(CL-*co*-41 mol % LA) components, T_g is a glass-transition temperature of the blend, and *k* is an empirical adjustable parameter. It has been concluded that bacterial P[(*R*)-3HB] is miscible with P(CL-*co*-41 mol % LA) (M_n = 18 000) in the melt. The blend of P[(*R*)-3HB] with P(CL-*co*-68 mol % LA) (sample 16) also showed a single T_g which depends on the blend composition. On the other hand, the blend of P[(*R*)-3HB] with PLA (sample 17) showed two T_g values. The

Table 3. Thermal Properties of P[(*R*)-3HB]/P(CL-*co*-LA) Blends

sample	blend comp, wt ratio	T_g,[a] °C		T_{cc},[b] °C	P(CL-*co*-LA)		P[(*R*)-3HB]		miscibility of blend[f]
					T_m,[c] °C	ΔH_m,[d] J/g	T_m,[c] °C	ΔH_m,[d] J/g	
P[(*R*)-3HB]		4		51			176	89	
P[(*R*)-3HB]/	75/25	nd[e]	3	50	59	61	164, 176	100	I
PCL	50/50	nd	5	48	59	101	164, 176	108	
$M_n = 22\,000$	25/75	nd	4	47	62	107	162, 176	104	
(sample 11)	0/100	−67		nd	60	110			
P[(*R*)-3HB]/	75/25	nd	4	46	46	58	163, 176	96	I
P(CL-*co*-9% LA)	50/50	nd	5	nd	nd	nd	174	96	
$M_n = 19\,000$	25/75	nd	3	nd	46	48	163, 174	112	
(sample 12)	0/100	−52		nd	48	53			
P[(*R*)-3HB]/	75/25	−42	3	44	nd	nd	161, 176	105	I
P(CL-*co*-18% LA)	50/50	nd	3	46	39	4	162, 175	112	
$M_n = 24\,000$	25/75	−50	nd	47	16, 37	11	162, 175	106	
(sample 13)	0/100	−48		nd	19	12			
P[(*R*)-3HB]/	75/25	−46	nd	nd	nd	0	162, 176	102	I
P(CL-*co*-21% LA)	50/50	−46	nd	nd	nd	0	162, 176	107	
$M_n = 23\,000$	25/75	−46	nd	nd	nd	0	162, 175	96	
(sample 14)	0/100	−45		nd	nd	0			
P[(*R*)-3HB]/	75/25	0		46	nd	0	162, 175	101	M
P(CL-*co*-41% LA)	50/50	−7		55	nd	0	158, 173	124	
$M_n = 18\,000$	25/75	−17		59	nd	0	158, 173	106	
(sample 15)	0/100	−23		nd	nd	0			
P[(*R*)-3HB]/	75/25	6		50	nd	0	162, 175	91	M
P(CL-*co*-68% LA)	50/50	6		53	nd	0	159, 174	128	
$M_n = 18\,000$	25/75	9		66	nd	0	157, 174	106	
(sample 16)	0/100	12		nd	nd	0			
P[(*R*)-3HB]/	75/25	nd	8	56	nd	0	162, 175	64	PM
PLA	50/50	34	12	59	nd	0	158, 174	94	
$M_n = 17\,000$	25/75	49	13	71	nd	0	160, 174	104	
(sample 17)	0/100	49		nd	nd	0			

[a] Glass-transition temperature; measured by DSC (second scan) from −100 to +200 °C at a rate of 20 °C/min. [b] Cold crystallization peak temperature; measured by DSC (second scan). [c] Melting temperature; measured by DSC (first scan), from 0 to 200 °C at a rate of 10 °C/min. [d] Enthalpy of fusion per gram of blend component. [e] Not detected. [f] I, M, and PM denote immiscible, miscible, and partially miscible blends in the melt, respectively.

low T_g value of the P[(*R*)-3HB] component increased from 4 to 13 °C with increasing PLA content, while the high T_g value of the PLA component decreased from 49 to 34 °C with increasing P[(*R*)-3HB] content, suggesting that the blends of P[(*R*)-3HB] with PLA ($M_n = 17\,000$) are partially miscible in the melt.

P[(*R*)-3HB], P(CL-*co*-9 mol % LA), and P(CL-*co*-18 mol % LA) are semicrystalline polymers with melting temperatures at 177, 48, and 19 °C, respectively. On the other hand, P(CL-*co*-LA) samples with 21−100 mol % of LA fraction are amorphous polymers. The solution-cast films of P[(*R*)-3HB]/P(CL-*co*-LA) blends exhibited two endotherm peaks of the P[(*R*)-3HB] component at temperatures of 157−176 °C (see Table 3). The high T_m values (173−176 °C) of the P[(*R*)-3HB] component in the blends remained nearly unchanged independent of blend composition. The lower T_m values of P[(*R*)-3HB] in the immiscible blends were in the range 161−164 °C, and those in the miscible blends were in the range 157−162 °C. Pearce and Marchessault[28] pointed out that the lower T_m of the P[(*R*)-3HB] component in the solution-cast films of P[(*R*)-3HB]/P[(*R,S*)-3HB] blends corresponded to the melting of the as-formed crystal and that the higher T_m reflected the remelting of the recrystallized crystal after melting of the as-formed crystal. As Table 3 shows, the T_m values of PCL in the immiscible P[(*R*)-3HB]/PCL blends were in the range 59−62 °C. An apparent correlation between the T_m values of the blend components and the miscibility of the blend was not observed for the solution-cast films of the blends. In addition, the ΔH_m values of P(CL-*co*-LA) and P[(*R*)-3HB] in both the miscible and immiscible blends were dependent on the blend composition. Thus, melting properties of the blend components could not be accounted for in terms of the miscibility of the blend.

As Table 3 shows, the cold crystallization peak temperatures (T_{cc}) of the P[(*R*)-3HB] component in the immiscible blends were 44−50 °C, independent of blend composition. In contrast, the T_{cc} values of the P[(*R*)-3HB] component in the miscible and partially miscible blends increased from 46 to 71 °C with an increase in the P(CL-*co*-LA) content. The increase in T_{cc} values observed for miscible blends can be explained considering that the crystallization process takes place from single homogeneous phase.[29]

Table 4 gives the thermal properties of the blends of P[(*R*)-3HB] ($M_n = 300\,000$) with amorphous P(CL-*co*-LA) of various molecular weights ($M_n = 1800−33\,000$). All quenched blend samples exhibited a single T_g which was dependent on the blend composition. The values of T_g were in good agreement with the curves calculated by the Wood's equation (1) with k values of 0.74, 0.82, 0.94, 0.78, and 0.74 for samples 4, 24, 8, 15, and 21, respectively. These results suggest that the blends of P[(*R*)-3HB] with P(CL-*co*-LA) ($M_n = 1800−33\,000$) containing ~40 mol % LA are miscible in the melt.

The miscibility of blends of P[(*R*)-3HB] ($M_n = 300\,000$) and P(CL-*co*-LA) with various copolymer compositions and molecular weights were determined from the T_g data of the blends. Figure 5 summarizes the effects of the copolymer composition and molecular weight of the P(CL-*co*-LA) component on the miscibility of the P[(*R*)-

Table 4. Thermal Properties of Blends of P[(*R*)-3HB] with P(CL-*co*-LA) Containing about 40 mol % LA

sample	blend comp, wt ratio	T_g,[a] °C	T_{cc},[b] °C	P[(*R*)-3HB] T_m,[c] °C	P[(*R*)-3HB] ΔH_m,[d] J/g	miscibility of blend[f]
P[(*R*)-3HB]		4	51	176	89	
P[(*R*)-3HB]/	75/25	−1	45	159, 175	100	
P(CL-*co*-45 % LA)	50/50	−6	52	151, 170	108	M
M_n = 1800	25/75	−18	47	147, 167	104	
(sample 4)	0/100	−24	nd			
P[(*R*)-3HB]/	75/25	nd[e]	nd	159, 175	96	
P(CL-*co*-41 % LA)	50/50	−11	62	153, 171	96	M
M_n = 6900	25/75	−18	57	151, 169	112	
(sample 24)	0/100	−28	nd			
P[(*R*)-3HB]/	75/25	−3	54	158, 175	105	
P(CL-*co*-41 % LA)	50/50	−7	54	153, 172	112	M
M_n = 17 000	25/75	−15	60	153, 170	106	
(sample 8)	0/100	−21	nd			
P[(*R*)-3HB]/	75/25	0	46	162, 175	101	
P(CL-*co*-41 % LA)	50/50	−7	55	158, 173	124	M
M_n = 18 000	25/75	−17	59	158, 173	106	
(sample 15)	0/100	−23	nd			
P[(*R*)-3HB]/	50/50	−9	57	159, 173	124	
P(CL-*co*-42 % LA)	25/75	−14	64	158, 173	132	M
M_n = 33 000	0/100	−23	nd			
(sample 21)						

[a] Glass-transition temperature; measured by DSC (second scan) from −100 to +200 °C at a rate of 20 °C/min. [b] Cold crystallization peak temperature; measured by DSC (second scan). [c] Melting temperature; measured by DSC (first scan), from 0 to 200 °C at a rate of 10 °C/min. [d] Enthalpy of fusion per gram of blend component. [e] Not detected. [f] I, M, and PM denote immiscible, miscible, and partially miscible blends in the melt, respectively.

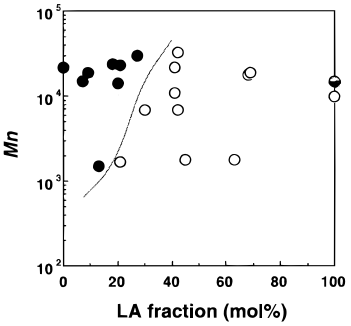

Figure 5. Effects of number-average molecular weight (M_n) and copolymer composition of P(CL-*co*-LA) component on the miscibility of P[(*R*)-3HB]/P(CL-*co*-LA) blends; miscible blend (○), partially miscible blend (◒); and immiscible blend (●).

3HB]/P(CL-*co*-LA) blend. In a previous paper,[17] we reported that the blend of P[(*R*)-3HB] (M_n = 300 000) with P[(*R,S*)-LA] (M_n = 9000) was miscible in the melt. As can be seen from Figure 5, the miscibility of P[(*R*)-3HB]/P(CL-*co*-LA) blends is strongly dependent on the copolymer composition of the P(CL-*co*-LA) component. The miscible blends of P[(*R*)-3HB] were prepared with amorphous P(CL-*co*-LA) ranging from 30 to 100 mol % LA. In addition, the miscibility of the blends was influenced by the molecular weight of the P(CL-*co*-LA) component. McCarthy[30] found that the blends of P[(*R*)-3HB] with PCL (M_n = 530) of low molecular weights were miscible.

The effect of the molecular weight of the P(CL-*co*-LA) component on the miscibility of the blends can be explained by the Flory−Huggins equation (2):[31]

$$\frac{\Delta G}{k_B T} = \frac{V}{V_r}\left(\frac{\phi_1}{n_1}\ln \phi_1 + \frac{\phi_2}{n_2}\ln \phi_2 + \chi_{12}\phi_1\phi_2\right) \qquad (2)$$

where ΔG is the change of free energy by mixing of two polymers, V is the volume of the mixing system, V_r is the molar volume of a segment, k_B is the Boltzmann constant, ϕ_1 and ϕ_2 are respectively volume fractions of P[(*R*)-3HB] and P(CL-*co*-LA), n_1 and n_2 are respectively the degrees of polymerization of P[(*R*)-3HB] and P(CL-*co*-LA), and χ_{12} is the Flory interaction parameter. When the M_n value of each polymer component is high enough, the first and second terms are negligible with respect to the third term, and ΔG is dependent on the χ_{12} parameter. In the P[(*R*)-3HB] (M_n = 300 000)/P(CL-*co*-21 mol % LA) blends, the change from immiscible to miscible with decreasing molecular weight can indicate a rather unfavorable value of the χ_{12} parameter, which is overrun only when the molecular weight is low enough, i.e., when the second term in eq 2 becomes significant. The result in Figure 5 suggests that the value of the χ_{12} parameter for the P[(*R*)-3HB]/P(CL-*co*-LA) blend decreases with increasing LA content in the P(CL-*co*-LA) component. When the M_n of the P(CL-*co*-LA) component is low, the second term is negative and competitive with the χ_{12} parameter.

Spherulite Morphology. The growth of P[(*R*)-3HB] spherulites in the P[(*R*)-3HB]/P(CL-*co*-LA) blends was observed with a polarized optical microscope. The samples were isothermally crystallized at a given temperature between 60 and 120 °C after melting at 200 °C for 30 s. Figures 6a−d show the radial growth rates (*G*) of P[(*R*)-3HB] spherulites at different crystallization temperatures in the blends of P[(*R*)-3HB] with P(CL-*co*-18 mol % LA), P(CL-*co*-41 mol % LA), P(CL-*co*-68 mol % LA), and PLA (samples 13, 15, 16, and 17), respectively. The spherulite radius increased linearly with time. The radial growth rate (*G*) was calculated as the slope of the line plotting the spherulite radius against time. A maximum value (3.4 μm/s) of *G* was observed near 90 °C for the P[(*R*)-3HB] homopolymer. As Figure 6a shows, the growth rate of P[(*R*)-3HB] spherulites in the immiscible P[(*R*)-3HB]/P(CL-*co*-18 mol % LA) blend was dependent on the crystallization temperature, while the rate was independent of the blend composition. In contrast, the *G* values decreased with an increase in the

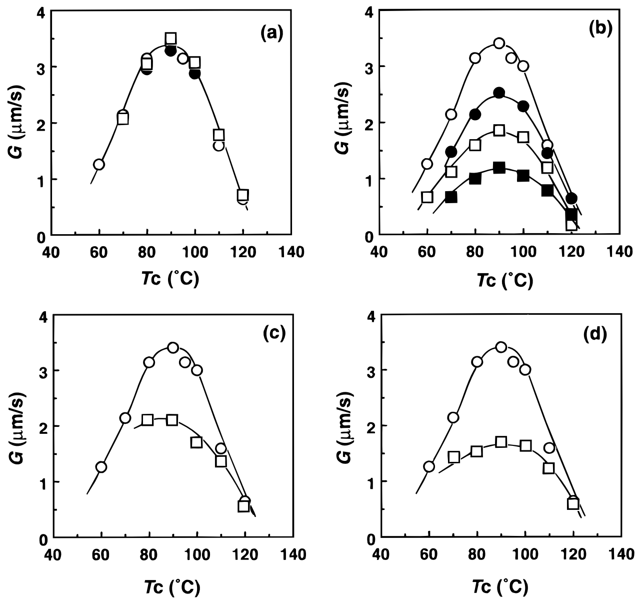

Figure 6. Radial growth rate (*G*) of P[(*R*)-3HB] spherulites as a function of crystallization temperature (T_c) for (a) P[(*R*)-3HB]/P(CL-*co*-18 mol % LA) (sample 13), (b) P[(*R*)-3HB]/P(CL-*co*-41 mol % LA) (sample 15), (c) P[(*R*)-3HB]/P(CL-*co*-68 mol % LA) (sample 16), and (d) P[(*R*)-3HB]/PLA (sample 17). Weight fractions of P[(*R*)-3HB]/P(CL-*co*-LA) blends are 100/0 (○), 75/25 (●), 50/50 (□), and 25/75 (■).

content of the P(CL-*co*-LA) component for the miscible blends of P[(*R*)-3HB] and P(CL-*co*-LA) with 41−100 mol % LA (see Figures 6b−d). The results suggest that the P(CL-*co*-LA) components with 41−100 mol % LA act as a diluent for crystallizable P[(*R*)-3HB]. The same results were obtained for the miscible blends of P[(*R*)-3HB] with atactic P[(*R,S*)-3HB][10,32] and with atactic P[(*R,S*)-LA].[17]

Figures 7a and 7b show typical optical micrographs of P[(*R*)-3HB] spherulites in immiscible and miscible blends of P[(*R*)-3HB]/P(CL-*co*-LA) 50/50 (w/w), respectively. After crystallization, the P[(*R*)-3HB] spherulites were well-developed throughout the blend films, suggesting that the uncrystallizable P(CL-*co*-LA) component exists within the spherulites of P[(*R*)-3HB]. In the miscible blend of P[(*R*)-3HB]/P(CL-*co*-41 mol % LA), the spherulites of P[(*R*)-3HB] exhibited obvious banding (see Figure 7b). However, the texture of P[(*R*)-3HB] spherulites was not apparent in the immiscible blend of P[(*R*)-3HB]/P(CL-*co*-18 mol % LA), and small particles were observed in P[(*R*)-3HB] spherulites (see Figure 7a). This suggests that the phase separation of the P[(*R*)-3HB] and P(CL-*co*-18 mol % LA) components occurred in interfibrillar regions within the P[(*R*)-3HB] spherulites.

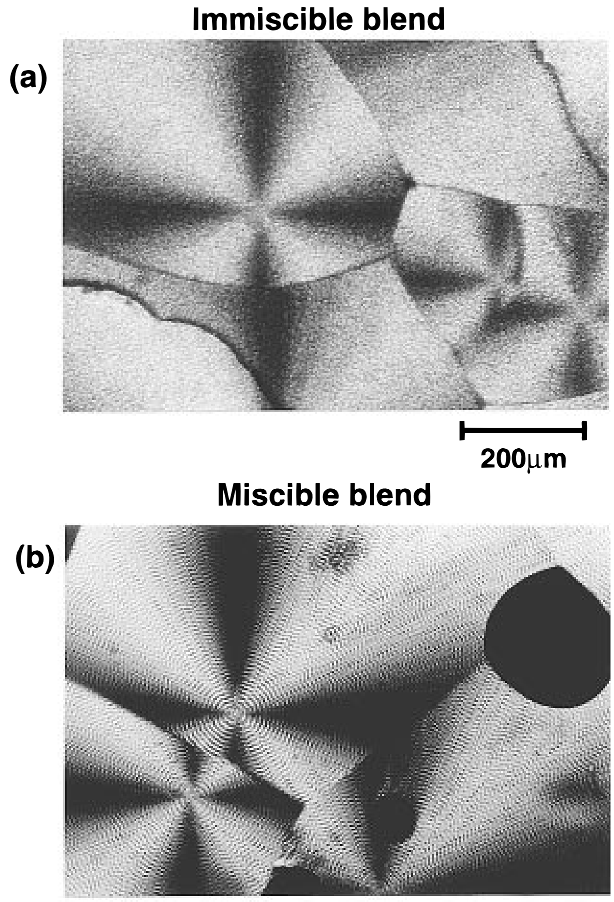

Figure 7. Optical micrographs of P[(*R*)-3HB] spherulites in the blend films of (a) P[(*R*)-3HB]/P(CL-*co*-18 mol % LA) [50/50 (w/w)] at T_c = 80 °C and (b) P[(*R*)-3HB]/P(CL-*co*-41 mol % LA) [50/50 (w/w)] at T_c = 100 °C.

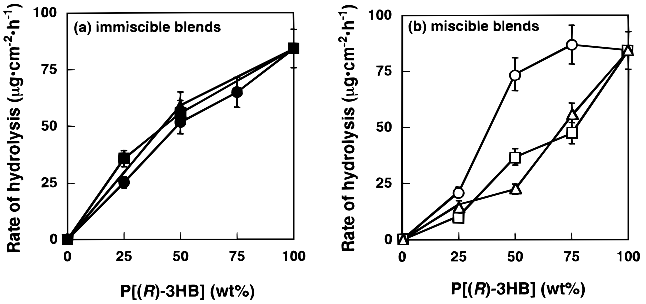

Figure 8. Effect of blend composition on the rates of enzymatic hydrolysis of P[(*R*)-3HB]/P(CL-*co*-LA) films in the aqueous solution of PHB depolymerase from *A. faecalis* at 37 °C and pH 7.4: (a) immiscible blends of P[(*R*)-3HB] with P(CL-*co*-9 mol % LA) (sample 12) (■), P(CL-*co*-18 mol % LA) (sample 13) (●), and P(CL-*co*-21 mol % LA) (sample 14) (▲); (b) miscible or partially miscible blends of P[(*R*)-3HB] with P(CL-*co*-41 mol % LA) (sample 15) (□), P(CL-*co*-68 mol % LA) (sample 16) (○), and PLA (sample 17) (△).

Biodegradation of P[(*R*)-3HB]/P(CL-*co*-LA) Blend Films. An extracellular PHB depolymerase from *A. faecalis* was used for the enzymatic hydrolysis of blend films. The enzymatic hydrolyses of solution-cast films of P[(*R*)-3HB]/P(CL-*co*-LA) blends were carried out for a given time between 3 and 19 h at 37 °C in a 0.1 M potassium phosphate solution (pH 7.4) of PHB depolymerase. The weight loss of films of P[(*R*)-3HB]/P(CL-*co*-LA) blends increased proportionally with time. The rate of enzymatic hydrolysis was determined from the slope of the line obtained by plotting the weight loss against time. Figures 8a and 8b show the rates of enzymatic hydrolysis of P[(*R*)-3HB]/P(CL-*co*-LA) blends. The effect of blend composition on the rate of hydrolysis for immiscible blends and miscible or partially miscible blends is given in Figures 8a and 8b, respectively. No weight loss was observed for the PLA and P(CL-*co*-LA) in the presence of PHB depolymerase. The rate of enzymatic hydrolysis increased with increasing P[(*R*)-3HB] content, since PHB depolymerase is capable of hydrolyzing polymer chains of P[(*R*)-3HB]. However, no apparent difference was observed for the rates of enzymatic hydrolysis on the films of immiscible and miscible polymer blends.

Figures 9a−d show the scanning electron micrographs (SEMs) of surfaces of blend films before and after enzymatic hydrolysis. The surface of miscible P[(*R*)-3HB]/P(CL-*co*-41 mol % LA) [50/50 (w/w)] blend film

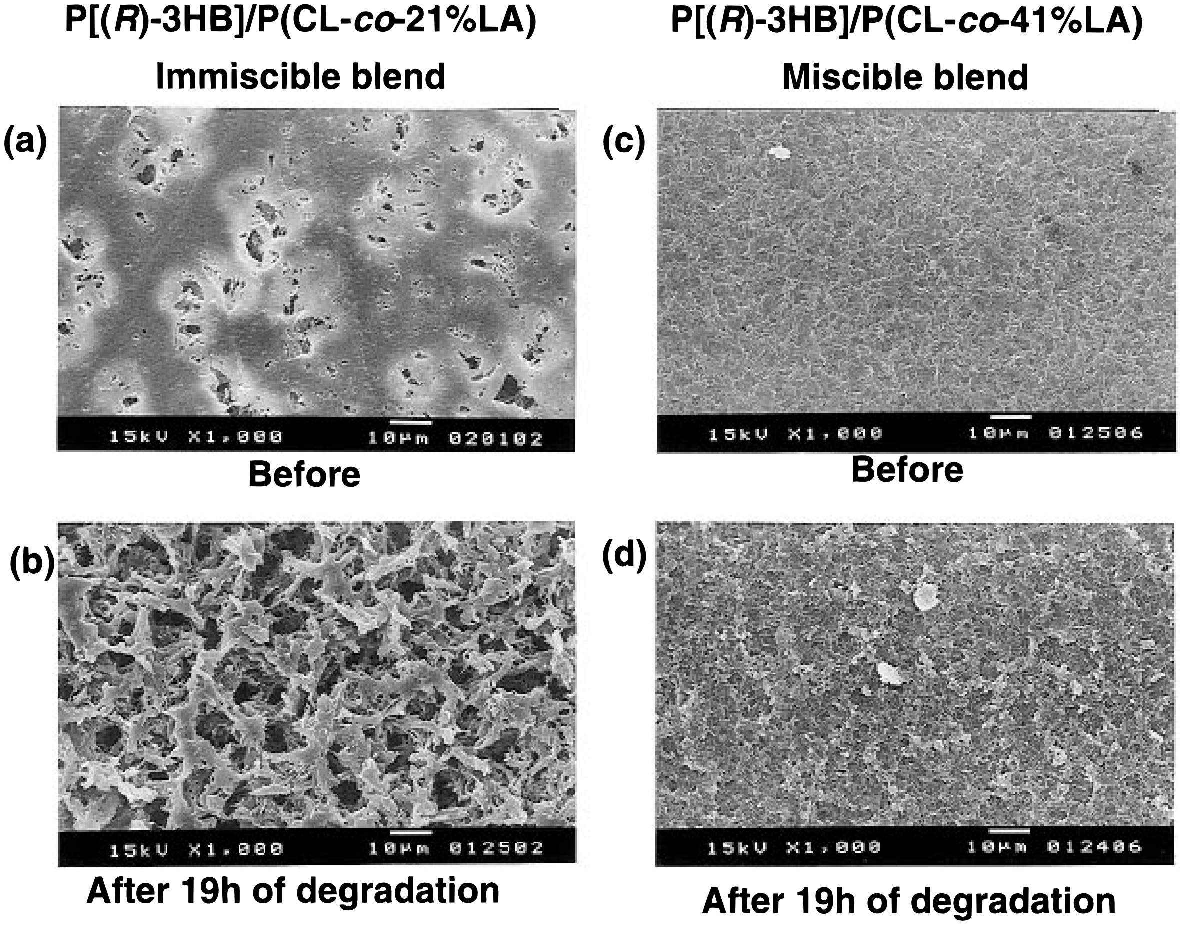

Figure 9. SEMs of the surfaces of blend films before and after enzymatic hydrolysis with PHB depolymerase: (a) and (b) P[(*R*)-3HB]/P(CL-*co*-21 mol % LA) [50/50 (w/w)]; (c) and (d) P[(*R*)-3HB]/P(CL-*co*-41 mol % LA) [50/50 (w/w)].

after enzymatic hydrolysis for 19 h was uniformly blemished by the action of PHB depolymerase (see Figure 9d), suggesting that the enzymatic hydrolysis took place on the surface of the films. In contrast, a number of holes of $\sim$10 μm in diameter were detected on the surface of immiscible P[(*R*)-3HB]/P(CL-*co*-21 mol % LA) [50/50 (w/w)] blend film after enzymatic hydrolysis for 19 h (see Figure 9b).

The biodegradation tests of P[(*R*)-3HB]/P(CL-*co*-LA) blend films were performed at 25 °C for 28 days under aerobic conditions in a natural water from the Arakawa river (Saitama, Japan) as an inoculum, by monitoring the time-dependent changes in the biochemical oxygen demand (BOD). Figure 10 shows the BOD biodegradation curves of the miscible blends of P[(*R*)-3HB] with P(CL-*co*-41 mol % LA) (sample 24). The BOD biodegradation of P[(*R*)-3HB] film increased with time to reach $\sim$80% biodegradability in 28 days. The rates of biodegradation for the P[(*R*)-3HB]/P(CL-*co*-41 mol % LA) blends were slightly lower than that of P[(*R*)-3HB]. The BOD biodegradabilities of blend films after 28 days were respectively 77 ± 2 and 62 ± 2% for 75/25 and 50/50 (w/w) of P[(*R*)-3HB]/P(CL-*co*-41 mol % LA). The weight loss biodegradabilities of P[(*R*)-3HB] and P[(*R*)-3HB]/P(CL-*co*-41 mol % LA) blends [75/25 (w/w)] and [50/50 (w/w)] were 100 ± 0, 100 ± 0, and 85 ± 5% after 28 days of test, respectively. In addition, the changes in the dissolved organic carbon concentration (DOC) of the test solution were measured before and after the biodegradation. The DOC values of test solution decreased from 2.8 mg C/L to 2.0 ± 0.2 mg C/L in 28 days for all samples. These results suggest that P[(*R*)-3HB]/P(CL-*co*-LA) blends are hydrolyzed to water-soluble products by the action of enzymes in the environment and that the majority of the products is utilized by microorganisms for energy generation and biomass formation.

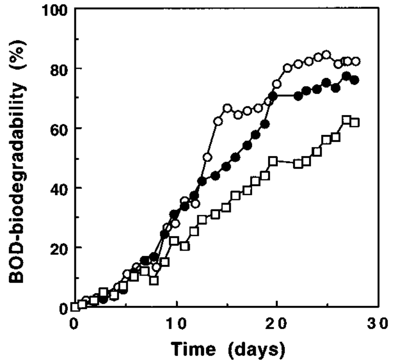

Figure 10. BOD biodegradation curves of the miscible blends of P[(*R*)-3HB] with P(CL-*co*-41 mol % LA) (sample 24) in Arakawa river water (Saitama, Japan) at 25 °C: P[(*R*)-3HB] (○); P[(*R*)-3HB]/P(CL-*co*-41 mol % LA) [75/25 (w/w)] (●); P[(*R*)-3HB]/P(CL-*co*-41 mol % LA) [50/50 (w/w)] (□).

Conclusion

Copolymers of ϵ-caprolactone (CL) and (*R*,*S*)-lactide (LA) with a wide range of compositions (0−100 mol % LA) and molecular weights (M_n = 1500−40 000) were prepared by ring-opening copolymerization of CL and LA at 70 °C for 5 days with aluminum triisopropoxide as an initiator. The P(CL-*co*-LA) samples had random sequence distributions of caprolactone and half-lactide (lactic acid) units. The P(CL-*co*-LA) samples with 0−18 mol % LA were partially crystalline, while those with 20−100 mol % LA were amorphous. The P(CL-*co*-LA) films were hydrolyzed at 37 °C by a lipase from *R. delemar*, and the rates of enzymatic hydrolysis were higher than the rate of PCL homopolymer.

The binary blends of bacterial poly[(*R*)-3-hydroxybutyric acid] (P[(*R*)-3HB]) ($M_n = 300\,000$) with biodegradable P(CL-*co*-LA) with a wide range of compositions and molecular weights were characterized by means of DSC and polarized optical microscopy. The miscibility of the blends was studied from the DSC thermograms recorded by heating samples of P[(*R*)-3HB]/P(CL-*co*-LA) blends quenched from 200 °C to liquid nitrogen temperature. When the M_n values of the P(CL-*co*-LA) component were ∼20 000, the blends of P[(*R*)-3HB] and P(CL-*co*-LA) with 0−21 mol % LA were immiscible in the melt, while the blends of P[(*R*)-3HB] and P(CL-*co*-LA) with 41−100 mol % LA were miscible or partially miscible. The blends of P[(*R*)-3HB] with P(CL-*co*-LA) containing ∼40 mol % LA were miscible, independent of molecular weight of the P(CL-*co*-41 mol % LA) component ranging in M_n values from 1500 to 33 000.

The P[(*R*)-3HB] spherulites were well-developed throughout the films of both immiscible and miscible blends of P[(*R*)-3HB]/P(CL-*co*-LA). The growth rates of P[(*R*)-3HB] spherulites were independent of the blend composition in the immiscible blends. In contrast, the spherulitic growth rates of P[(*R*)-3HB] in the miscible blends were dependent on the blend composition and decreased with increasing content of the P(CL-*co*-LA) component.

The films of P[(*R*)-3HB]/P(CL-*co*-LA) blends were hydrolyzed at 37 °C by PHB depolymerase from *A. faecalis*, and the rates of enzymatic hydrolysis decreased with increasing P(CL-*co*-LA) content, independent of the miscibility of the blend. The biodegradation of P[(*R*)-3HB]/P(CL-*co*-41 mol % LA) blends was conducted at 25 °C for 28 days in Arakawa river water (Saitama, Japan), and the blends were found to be degraded and utilized by microorganisms for energy generation and biomass formation.

Acknowledgment. We thank Mr. A. Mizuki for his skillful analysis measurements. This study was performed as a part of the development of Biodegradable Plastics supported by the New Energy and Industrial Technology Development Organization (NEDO).

References and Notes

(1) Dawes, E. A.; Senior, P. J. *Adv. Microb. Physiol.* **1973**, *10*, 135.

(2) Doi, Y. *Microbial Polyesters*; VCH Publishers: New York, 1990.

(3) Marchessault, R. H.; Coulombe, S.; Morikawa, H.; Okamura, K.; Revol, J. F. *Can. J. Chem.* **1981**, *59*, 38.

(4) Avella, M.; Martuscelli, E. *Polymer*, **1988**, *29*, 1731.

(5) Kumagai, Y.; Doi, Y. *Polym. Degrad. Stab.* **1992**, *35*, 87.

(6) Scandola, M.; Ceccorulli, G.; Pizzoli, M. *Macromolecules* **1992**, *25*, 6441.

(7) Ceccorulli, G.; Pizzoli, M.; Scandola, M. *Macromolecules* **1993**, *26*, 6722.

(8) Pearce, R.; Jesudason, J.; Orts, W.; Marchessault, R. H.; Bloembergen, S. *Polymer* **1992**, *33*, 4647.

(9) Kumagai, Y; Doi, Y. *Makromol. Chem., Rapid Commun.* **1992**, *13*, 179.

(10) Abe, H.; Doi, Y.; Satokowski, M. M.; Noda, I. *Macromolecules* **1994**, *27*, 50.

(11) Holland, S. J.; Tighe, B. J.; Gould, P. L. *J. Controlled Release* **1986**, *4*, 155.

(12) Reeve, M. S.; McCarthy, S. P.; Downey, M. J.; Gross, R. A. *Macromolecules* **1994**, *27*, 825.

(13) Fukuzaki, H.; Yoshida, M.; Asano, M.; Kumakura, M. *Eur. Polym. J.* **1989**, *25*, 1019.

(14) Pitt, C. G. In *Biodegradable Polymers and Plastics*; Vert, M., Feijen, J., Albertsson, A., Scott, G., Chiellini, E., Eds.; The Royal Society of Chemistry: Cambridge, 1991; p 7.

(15) Tokiwa, Y.; Ando, T.; Suzuki, T. *J. Ferment. Technol.* **1976**, *54*, 603.

(16) Kumagai, Y.; Doi, Y. *Polym. Degrad. Stab.* **1992**, *36*, 241.

(17) Koyama, N.; Doi, Y. *Can. J. Microbiol.* **1995**, *41* (Suppl. 1), 316.

(18) Vion, J. M.; Jerome, R.; Teyssie, P.; Aubin, M.; Prud'homme, R. E. *Macromolecules* **1986**, *19*, 1828.

(19) Vanhoorne, P.; Dubois, P.; Jerome, R.; Teyssie, P. *Macromolecules* **1992**, *25*, 37.

(20) Reeve, M. S.; McCarthy, S. P.; Gross, R. A. *Macromolecules* **1993**, *26*, 888.

(21) Tanio, T.; Fukui, T.; Shirakura, Y.; Saito, T.; Tomita, K.; Kaiho, T.; Masamune, S. *Eur. J. Biochem.* **1982**, *124*, 71.

(22) Yakabe, Y.; Kitano, M. In *Biodegradable Plastics and Polymers*; Doi, Y., Fukuda, K., Eds.; Elsevier: Amsterdam, 1994; p 331.

(23) Kasperczyk, J.; Bero, M. *Makromol. Chem.* **1991**, *192*, 1777.

(24) Kasperczyk, J.; Bero, M. *Makromol. Chem.* **1993**, *194*, 913.

(25) Mukai, K.; Doi, Y.; Sema, Y.; Tomita, K. *Biotechnol. Lett.* **1993**, *15*, 601.

(26) Abe, H.; Doi, Y.; Aoki, H.; Akehata, T.; Hori, Y.; Yamaguchi, A. *Macromolecules* **1995**, *28*, 7630.

(27) Wood, L. A. *J. Polym. Sci.* **1958**, *28*, 319.

(28) Pearce, R.; Marchessault, R. H. *Polymer* **1994,** *35*, 3990.

(29) Siciliano, A.; Seves, A.; De Marco, T.; Cimmino, S.; Martuscelli, E.; Silvestre, C. *Macromolecules* **1995**, *28*, 8065.

(30) McCarthy, P. J., personal communication.

(31) Flory, P. J. *Principles of Polymer Chemistry*; Cornell University Press: Ithaca, NY, 1953.

(32) Abe, H.; Matsubara, I.; Doi, Y. *Macromolecules* **1995**, *28*, 844.

MA960119L